

Critical role for CCR2 and HMGB1 in induction of experimental endotoxic shock



Jackson Nogueira Alves^{a,1}, Karla Maria Pereira Pires^{a,1}, Manuella Lanzetti^a, Marina Valente Barroso^b, Cláudia Farias Benjamim^b, Cristiane Aguiar Costa^c, Angela Castro Resende^c, Juliana Carvalho Santos^d, Marcelo Lima Ribeiro^d, Luís Cristóvão Porto^a, Samuel Santos Valença^{b,*}

^a Pós-graduação em Biologia Humana e Experimental, Instituto de Biologia Roberto Alcântara Gomes, Universidade do Estado do Rio de Janeiro, R.J., Brazil

^b Instituto de Ciências Biomédicas, Universidade Federal do Rio de Janeiro, R.J., Brazil

^c Departamento de Farmacologia e Psicobiologia, Instituto de Biologia Roberto Alcântara Gomes, Universidade do Estado do Rio de Janeiro, R.J., Brazil

^d Unidade de Farmacologia e Gastroenterologia, Universidade São Francisco de Assis, S.P., Brazil

ARTICLE INFO

Article history:

Received 16 April 2013

and in revised form 20 June 2013

Available online 3 July 2013

Keywords:

Sepsis

HMGB1

CCR2

MCP-1

Glycyrrhizic acid

ABSTRACT

Our aim was to investigate CCR2 and HMGB1 involvement in a murine model of endotoxic shock. We used C57BL/6 CCR2 knockout (KO) mice and wild-type (WT) littermates to establish an optimal dose of LPS. CCR2 KO mice survived more frequently than WT mice after 80, 40 and 20 mg/kg of LPS i.p. Inflammation and redox markers were high in WT mice than in CCR2 KO mice. HMGB1 expression was reduced in CCR2 KO mice in parallel to ERK 1/2 activation. Therefore, we used glycyrrhizic acid (50 mg/kg), an HMGB1 inhibitor in WT mice injected with LPS, and mortality was fully abolished. Thus, drugs targeting CCR2 and HMGB1 could represent future resources for sepsis treatment.

© 2013 Elsevier Inc. All rights reserved.

Introduction

Sepsis is a systemic inflammatory syndrome that leads to lethal damage to organs [1]. Sepsis is the second most prevalent cause of non-cardiac mortality in intensive care units, with death rates ranging from 20% to 50%, and the lung is the most frequent site of infection, with 44% incidence [2]. The initial stimulus for sepsis is an infection that generates a broad response within an organism, generally an unregulated manner [3]. Signs of sepsis found in humans, such as fever and lethargy, can also be observed in rodents by infection involving bacterial peritonitis, caecal perforation and connection, among other models of pneumonia [4]. Gram-negative bacteria are responsible for approximately 60% of sepsis cases [5]. In laboratory animals, lipopolysaccharide (LPS)² from *Escherichia coli* is frequently used as a model of sepsis [6,7]. LPS (also known as endotoxin) is located on the outer membrane of Gram-negative

bacteria and plays an important role in the release of proinflammatory mediators, the activation of nuclear factors (such as NFκB and AP-1) and the imbalance between oxidants and antioxidants [8,9].

Monocyte chemoattractant protein-1 (MCP-1) is a member of the CC chemokine subfamily and a potent chemotactic factor for monocytes [10]. The contribution of MCP-1 signalling through its receptor CCR2 in monocyte adhesion to inflamed endothelium during sepsis is not fully understood. Another protein not fully understood in sepsis is a highly mobile protein (HMGB1) that is secreted by macrophages, dendritic cells, and tumour endothelial cells and released in the necrosis process and has been reported as a “late proinflammatory mediator in sepsis”, the secretion of which can be detected from 8 to 32 h after endotoxaemia [11–13]. Patients with sepsis have elevated serum levels of HMGB1, and these levels are associated with increased mortality, suggesting that clinical intervention by blocking or neutralising HMGB1 could be a viable option [14–16]. HMGB1 can induce the activation of intracellular signalling pathways through interactions with at least three pathways of recognising receptor patterns: activation of toll-like receptor types 2 and 4 and receptor for advanced glycation end products [17]. Thus, extracellular HMGB1 works synergistically with other pro-inflammatory mediators to induce responses of innate immunity [18–21].

In the present study, we investigated LPS-induced endotoxic shock with respect to the MCP-1/CCR2 response by time and dose.

* Corresponding author. Address: ICB/CCS/UFRJ. Av. Carlos Chagas Filho 373 Bloco F/sala14. Ilha do fundão, Rio de Janeiro, R.J., CEP 21.941-902, Brazil. Fax: +55 21 25 62 64 60.

E-mail address: samueltv@ufrj.br (S.S. Valença).

¹ These authors contributed equally to this work.

² Abbreviations used: LPS, lipopolysaccharide; MCP-1, monocyte chemoattractant protein-1; HTAB, hexadecyltrimethylammonium bromide; TMB, tetramethylbenzidine; GA, glycyrrhizic acid; BAL, bronchoalveolar lavage; ROS, reactive oxygen species; MPO, Myeloperoxidase

Furthermore, we analyse HMGB1 involvement through histological, redox and inflammatory profiles.

Material and methods

Reagents

The following reagents were purchased from Sigma Chemical (St. Louis, MO, USA): acrylamide, bovine serum albumin, eosine, glycyrrhizic acid, hematoxylin, hexadecyltrimethylammonium bromide (HTAB), lipopolysaccharide from *Escherichia coli* strain 0111:B4, myeloperoxidase, naphthylendiamide dihydrochloride, nitroblue tetrazolium, sodium acetate buffer, sodium chloride, sodium dodecylsulphate, sodium nitrite, sulphanilamide and 3,30,5,50-tetramethylbenzidine (TMB). Bradford assay reagents were purchased from Bio-Rad (Hercules, CA, USA). Formalin, hydrogen peroxide and phosphoric acid were purchased from Vetec (Duque de Caxias, Rio de Janeiro, Brazil).

Animals

Male C57BL/6 (wild type; WT) and CCR2-deficient mice (CCR2^{-/-}), 8–10 weeks old, were bred and maintained under standard conditions in the animal facility of the Institute of Biomedical Science, Federal University of Rio de Janeiro (Rio de Janeiro, Brazil). The CCR2^{-/-} mice were generated by W.A. Kuziel [22] and were kindly supplied. These CCR2^{-/-} mice were backcrossed with C57BL/6 mice for over 20 generations. All of the procedures were in accordance with international guidelines (NIH) and Brazilian law (the “Arouca” Law) for the use of animals (Law 11,794 from 10/08/2008), and this study received prior approval from the animal ethics committee of the Federal University of Rio de Janeiro (IBCCF 108). During the experiment, the animals had controlled temperature and humidity (21 ± 2 °C, 50 ± 10%, respectively) and were subjected to 12 h light/dark cycles. During the experimental procedures, the animals received standard chow and water ad libitum.

Experimental design

To establish an optimal LPS concentration in mice, we performed a dose–response study, using *E. coli* strain 0111:B4 to induce endotoxic shock. LPS was suspended in saline, sonicated at 30 °C for 15 min before use and inoculated i.p. at concentrations of 20, 40 and 80 mg/kg in WT and KO animals (*n* = 10 each group). The animals were monitored for 24 h after the inoculation of LPS, and the mortality of each group was computed. The animals subjected to endotoxaemia primarily developed signs of sepsis, such as piloerection (suggesting hyperthermia), lethargy, and increased respiratory and heart rates. At the end of the experimental design, we established the optimal dose of 20 mg/kg of animal after obtaining 70% survival of the mice, and subsequent analyses were performed only in these mice. A second experimental design was performed with C57BL/6 mice (*n* = 10 each group) and monitored for 24 h. One hour after LPS inoculation (i.p.), these mice were treated with saline or 50 mg/kg glycyrrhizic acid (GA), an HMGB1 inhibitor. The groups were defined as Control, GA, LPS and LPS + GA. In order to study survival improvements by GA administration, the following groups were analysed: LPS, LPS + GA, LPS KO and LPS KO + GA.

Bronchoalveolar lavage

The lung air spaces were washed three times with buffered saline solution (500 µL) for a final bronchoalveolar lavage (BAL) fluid

volume of 1.2–1.5 mL. The collected BAL fluid was stored on ice. The total number of cells in the BAL fluid was determined using a Neubauer chamber. After BAL, the lungs were removed immediately, homogenised on ice with 10% (w/v) 0.1 M potassium phosphate buffer (pH 7.4) using a tissue homogeniser (Nova técnica homogeniser model NT136, Campinas, São Paulo, Brazil), and centrifuged at 800 g for 5 min. The supernatants were stored at 20 °C for biochemical analysis. The protein concentration in the lung homogenate samples was determined by the Bradford method [23].

ROS assay

We used a nitroblue tetrazolium assay to determine the reactive oxygen species (ROS) production in the leukocytes from the BAL by the method adapted from Choi and colleagues [24].

Myeloperoxidase (MPO) assay

MPO activity was measured using hydrogen peroxide, HTAB, and TMB. Initially, 100 µL of each BAL sample was centrifuged with 900 µL of HTAB at 14,000 g for 15 min. The supernatant (75 µL) was incubated with 5 µL of TMB for 5 min at 37 °C. The mixture was then incubated with 50 µL of hydrogen peroxide for 10 min at 37 °C, after which 125 µL of sodium acetate buffer was added. The reaction was read using a microplate reader (Bio-Rad model 550, Hercules, CA, USA) at 630 nm [25]. The concentration of MPO in the samples was determined using a standard curve established using purified MPO.

Nitrite content

The nitrite levels in the lung homogenates were determined by a method based on the Griess reaction [26]. A total of 100 µL of sample was mixed with 100 µL of Griess reagent (1% sulphanilamide in 5% phosphoric acid and 0.1% naphthylendiamide dihydrochloride in water) and incubated at room temperature for 10 min. The absorbance was measured with a plate reader at 550 nm. The nitrite concentrations in the samples were determined from a standard curve generated using different concentrations of purified sodium nitrite.

Histopathology

Twenty-four hours after LPS administration, a separated group of mice were killed, and after a midline thoracotomy, the trachea was cannulated, and the lungs were fixed by the instillation of 0.5 ml of buffered formalin (10%) at a pressure of 18–22 cmH₂O for 1–2 min. The trachea was then ligated, and the lungs, kidney and liver were immersed in the fixative solution for 48 h. The organs were embedded in paraffin, sliced (5 µm) and stained with H&E.

RNA extraction and quantitative real-time PCR

Lung tissue fragments were collected, snap frozen, and stored at –80 °C in RNA later (Qiagen, Valencia, CA, USA). The total RNA was isolated using the RNeasy tissue kit (Qiagen). Single-stranded cDNA was synthesised using the High Capacity cDNA Archive Kit (Applied Biosystems, Foster City, CA, USA) according to the manufacturer's protocol. Quantitative real-time PCR was performed using a 7300 real-time PCR System (Applied Biosystems), and the threshold cycle numbers were determined using the RQ Study Software (Applied Biosystems). The reactions were performed in triplicate, and the threshold cycle numbers were averaged. The 50 µL reaction mixture was prepared as follows: 25 µL of Platinum SYBR

Green Quantitative PCR SuperMix-UDG (Invitrogen Life Technologies, Alameda, CA, USA), 10 $\mu\text{mol/L}$ of each primer (Table 1) and 10 μL of cDNA (100 ng). The reaction was cycled with a preliminary uracil–DNA glycosylase treatment for 2 min at 50 °C and a denaturation step for 2 min at 95 °C, followed by 45 cycles of denaturation at 95 °C for 15 s, annealing for 15 s, and primer extension at 72 °C for 15 s. This process was followed by melting point analysis of the double-stranded amplicons, consisting of 40 cycles of 1 °C decrements (15 s each) beginning at 95 °C. The first derivative of this plot, dF/dT , is the rate of change of fluorescence in the reaction, and a significant change in fluorescence accompanies the melting curve of the double-stranded PCR products. A plot of $-dF/dT$ vs. temperature displays these changes as distinct peaks. Thus, iNOS, MCP-1, TNF- α , CCR2, TLR4, NRF2, and SIRT1 expression were examined and normalised to a constitutive gene (β -actin and HRPT-1), and the relative fold induction was calculated according to the formula $2^{(-\Delta\Delta Ct)}$ [27].

Western blotting

Samples of lung homogenates and BAL were mixed with Laemmle sample buffer and boiled for 5 min. Equal amounts of proteins (50 $\mu\text{g/sample}$) were resolved by 8% sodium dodecyl sulphate–polyacrylamide gel electrophoresis, and transferred onto polyvinylidene fluoride (PVDF) membranes (Bio-Rad, Hercules, CA, USA). The membranes were probed with specific antibodies and dilutions: HMGB1 (1:1,000), ERK 1/2 (1:1,000) and pERK 1/2 (1:1,000); β -actin (1:1,000) served as the endogenous control. Detection was observed with HRP-conjugated goat anti-rabbit IgG secondary antibody. The bands were visualised by enhanced chemiluminescence (Amersham™ ECL™ Prime Western Blotting Detection Reagent, Pittsburgh, PA, USA) and quantified using the ImageJ free software. HMGB1 was detected in BAL, whereas ERK 1/2 and pERK 1/2 were detected in the lung homogenates. All of the experiments were performed in triplicate.

Elisa

Samples of BAL from mice injected with LPS or saline and treated with GA or saline were used for dosage of CCR2, HMGB1 and

MCP-1 measured using ELISA kits (MyBioSource Inc., San Diego, CA; Chondrex, Redmond, WA; R&D, Minneapolis, MN-USA).

Statistical Analyses

The data are presented as the means \pm standard error of the means and were analysed by the Student *t* test with Welch's correction, with $p < 0.05$. The symbols show the values of significance

Table 1
The primers used in the quantitative real-time PCR.

Gene	Primer	Sequence (5' → 3')
iNOS	Sense	CCGGAGAGGAGACTTCACAG
	Antisense	TCCACGATTCCAGAGAAC
MCP-1	Sense	ATTCTCCACACCTGTTCG
	Antisense	GATTCCTGGAAGGTGGTCAA
TNF- α	Sense	TAGCCAGGAGGAGAACAGA
	Antisense	TTTTCTGGAGGAGATGTGG
CCR2	Sense	ATTCTCCACACCTGTTCG
	Antisense	GATTCCTGGAAGGTGGTCAA
TLR4	Sense	GCTTTCACCTCTGCCTCAC
	Antisense	GCGATACAATCCACCTGCT
NRF2	Sense	TCTCCTCGCTGAAAAAGAA
	Antisense	AATGTGCTGGCTGTCTTTA
SIRT1	Sense	TGGCAAAGGAGCAGATTAGT
	Antisense	CTGCCACAAGAACTAGAGGA
β -actin	Sense	GCTACAGCTTCACCACCACA
	Antisense	TCTCCAGGGAGGAAGAGGAT
HRPT-1	Sense	GCTACAGCTTCACCACCACA
	Antisense	TCTCCAGGGAGGAAGAGGAT

iNOS, inducible isoform of nitric oxide synthase; MCP-1, monocyte chemoattractant protein-1; TNF- α , tumour necrosis factor alpha; CCR2, chemokine (C-C motif) receptor 2; TLR4, toll-like receptor 4; NRF2, nuclear factor (erythroid-derived 2)-like 2; SIRT1, sirtuin (silent mating type information regulation 2 homolog) 1; HRPT-1, hypoxanthine phosphoribosyl-transferase 1.

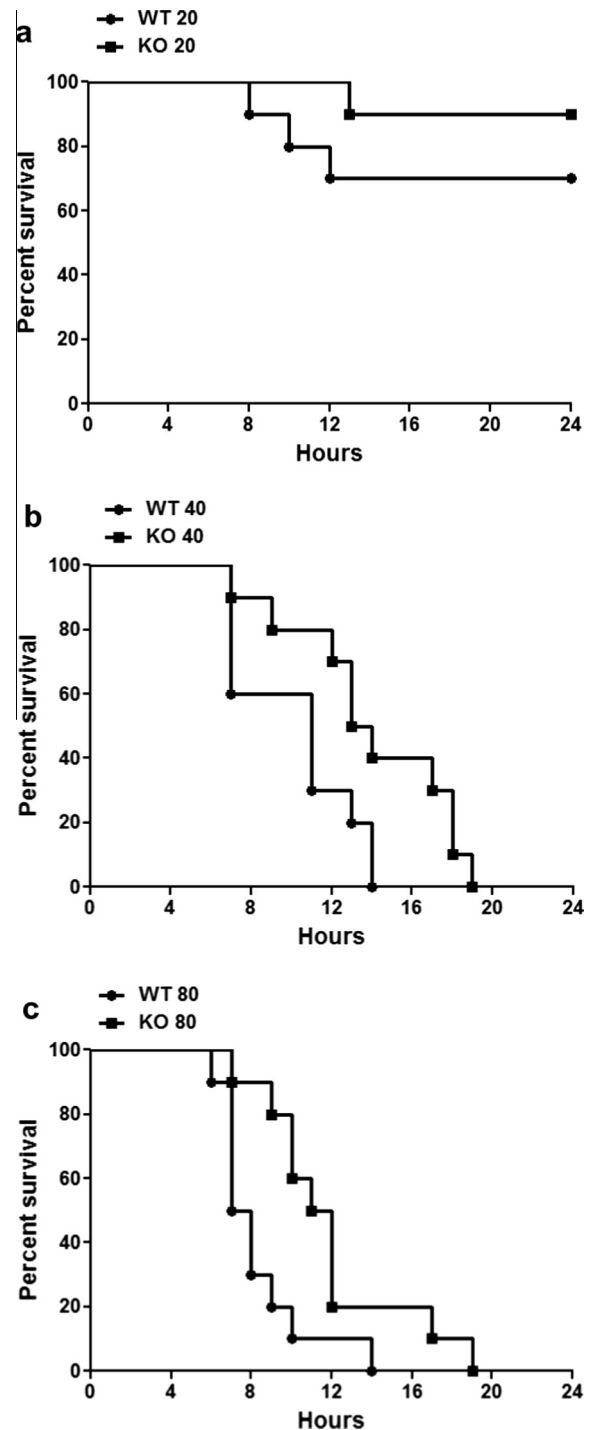


Fig. 1. Three doses of LPS i.p. were tested to assess mouse survival, 20 (a), 40 (b) and 80 mg/kg (c). Although CCR2 KO mice died when treated with 40 and 80 mg/kg of LPS, the WT mice died sooner. We chose to conduct our other analyses only in mice injected with 20 mg/kg of LPS i.p. These experimental designs were repeated three times. ($n = 10$ per group/time point).

$p < 0.001$, $p < 0.01$ and $p < 0.05$. The software GraphPad Prism 5 was used for statistical analysis (GraphPad Prism version 5.0, San Diego, CA, USA).

Results

LPS-induced lethality is reduced in CCR2 KO mice

We tested three doses of LPS i.p. to check CCR2 involvement in mice survival, 20 mg/kg (Fig. 1a), 40 mg/kg (Fig. 1b) and 80 mg/kg (Fig. 1c). Although CCR2 KO mice deaths were observed in groups injected with 40 and 80 mg/kg of LPS, the WT mouse deaths began sooner. We choose to perform our other analyses only in mice injected with 20 mg/kg of LPS i.p.

LPS-induced inflammatory and redox markers are altered in CCR2 KO mice

We observed increased leukocyte influxes in the BAL of both WT mice (threefold, $p < 0.001$) and CCR2 KO mice (twofold, $p < 0.001$) injected with LPS, compared with their respective control groups (Fig. 2a). The ROS in the BAL also increased in both WT mice (almost 200%, $p < 0.05$) and CCR2 KO mice (150%, $p < 0.05$) injected with LPS, compared with their respective control

groups (Fig. 2b). The MPO in the BAL, an indirect method for neutrophil quantification, was increased in both WT mice ($p < 0.001$) and CCR2 KO mice ($p < 0.001$) injected with LPS, compared with their respective control groups (Fig. 2c). Finally, the nitrite was measured in lung homogenates, and we observed an increase in WT mice ($p < 0.05$) injected with LPS compared with control group (Fig. 2d). The nitrite levels in the CCR2 KO mice injected with LPS were no different from those of the control group.

LPS-induced endotoxic shock damaged lung, kidney and liver

Lung-related sepsis is common, but for a 24 h experimental design, it is not the cause of death. We look then for other organs, such as the kidney and liver. We observed congestion, haemorrhage and leukocytes on the lung parenchyma in WT mice (Fig. 3b) injected with LPS compared with the control group (Fig. 3a). The lung histology of CCR2 KO mice (Fig. 3d) injected with LPS was not different from that of the control group (Fig. 3c). The kidneys of WT mice (Fig. 3f) injected with LPS showed that the renal tubular cells underwent significant vacuolar degenerative changes and leukocyte infiltrations in the glomeruli and interstitium compared with the control group (Fig. 3e). CCR2 mice injected with LPS (Fig. 3h) showed lesser kidney leukocyte infiltrations and no vacuolar degenerative changes compared with WT mice

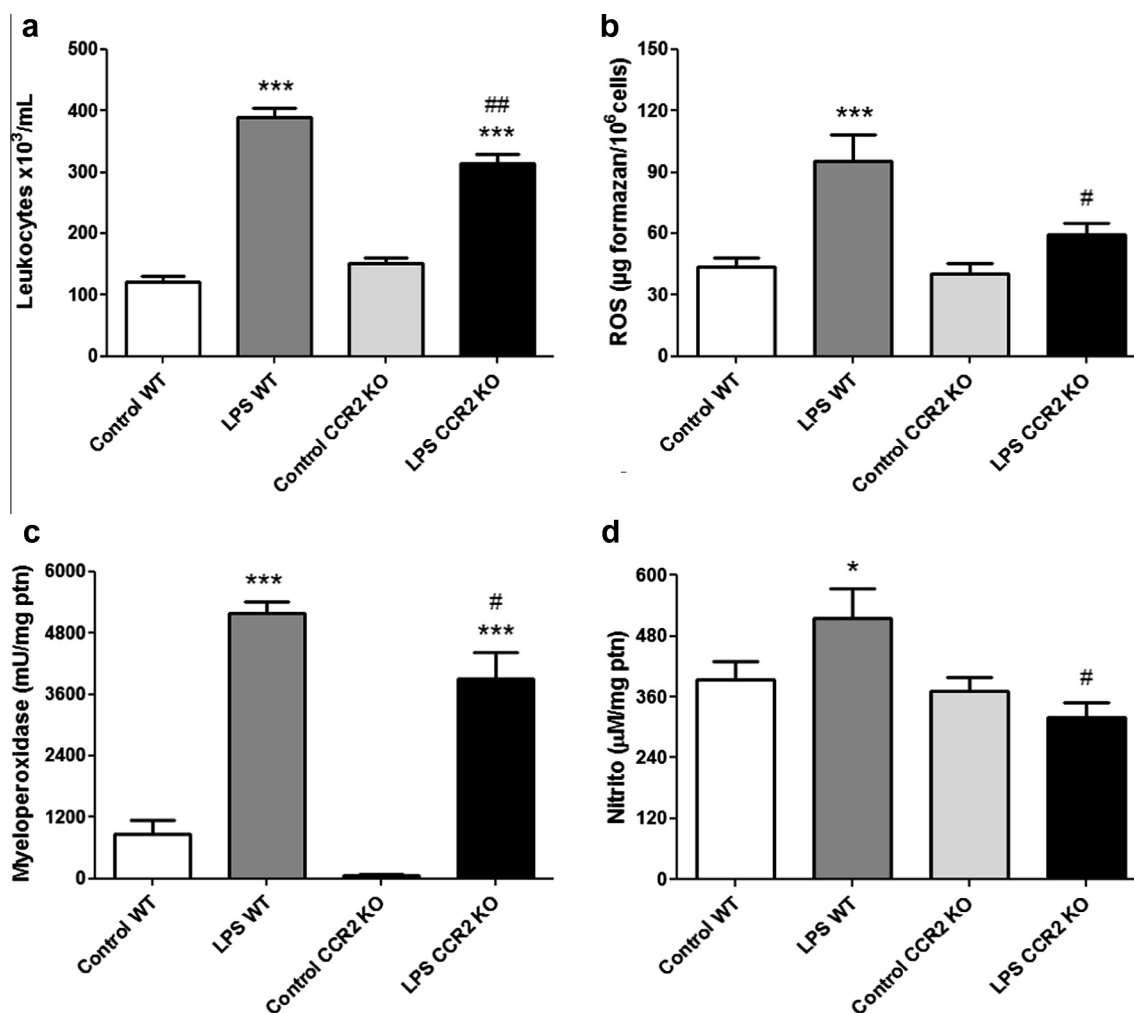


Fig. 2. Leukocytes and redox markers from lung and bronchoalveolar lavage or tissue of mice injected with LPS (20 mg/kg). (a) Total cells, (b) Reactive oxygen species, (c) Myeloperoxidase, and (d) Nitrite. The data were expressed as the means \pm SEM. The statistical analyses were performed by unpaired Student *T* tests with Welch's correction, considering the significance level to be 5%. * $p < 0.05$ and *** $p < 0.001$ compared with the respective control group. # $p < 0.05$ and ## $p < 0.01$ compared with LPS WT. Nitrite was measured in lung homogenates. The other measurements were performed in the BAL. $n = 10$ per group.

(Fig. 3g). The liver tissue of WT mice (Fig. 3j) injected with LPS showed wide-range laminated necrosis, acidophilia changes, and parenchyma leukocyte infiltrations compared with the control group (Fig. 3i). Liver tissue from CCR2 mice injected with LPS (Fig. 3l) showed only lesser parenchyma leukocyte infiltrations compared with the control group (Fig. 3k).

LPS-induced expression of inflammatory and redox markers is altered in CCR2 KO mice

We observed an increase in iNOS mRNA in the LPS-injected groups WT ($p < 0.05$) and CCR2 KO ($p < 0.05$) compared with controls (Fig. 4a). The mRNA of MCP-1 was also increased in the WT mice ($p < 0.05$) compared with the control group. However, MCP-1 mRNA was reduced in CCR2 KO mice (Fig. 4b) injected with LPS compared with the control group ($p < 0.01$). The expression of TNF- α was increased in both LPS-injected groups, WT ($p < 0.01$) and CCR2 KO ($p < 0.05$), compared with controls (Fig. 4c). CCR2 expression was observed only in WT mice, and those injected with LPS showed an increase in the mRNA ($p < 0.001$) compared with the control group (Fig. 4d). Toll 4 receptor expression was also increased in both LPS-injected groups, WT and CCR2 KO ($p < 0.05$ for both), compared with controls (Fig. 4e). The expression of the redox markers NRF2 (Fig. 4f) and SIRT1 (Fig. 4g) was reduced in LPS-injected mice, both WT ($p < 0.05$) and CCR2 ($p < 0.05$), compared with controls. The reduction in SIRT1 was less pronounced in CCR2 ($p < 0.05$) than in WT mice ($p < 0.01$).

LPS-induced endotoxic shock via ERK and HMGB1

We observed an increase in HMGB1 expression in the BAL from WT mice ($p < 0.001$) injected with LPS in comparison with the control group, whereas CCR2 KO mice injected with LPS were similar to their respective control group (Fig. 5). At the same time point,

we observed an increase in pERK 1/2 parallel to a reduction in ERK 1/2 in WT mice injected with LPS (Fig. 5). The pERK 1/2: ERK 1/2 ratio in CCR2 KO mice injected with LPS was similar to that of the respective control group (Fig. 5).

HMGB1 inhibition blocked mouse mortality after LPS-induced endotoxic shock

Until now, we observed that CCR2 is critical for mouse survival after LPS. It appears that HMGB1 signalling was altered by CCR2 KO via the ERK 1/2 pathway. Therefore, we used glycyrrhizic acid (GA), an HMGB1 inhibitor, as a target to reduce the impact of endotoxic shock caused by LPS. We observed that 100% of LPS + GA mice were alive at 24 h of experimental design, whereas 30% of the LPS mice were dead (Fig. 6). CCR2 KO mice subjected to endotoxic shock were 90% protected from death, whereas the survival rate of CCR2 KO + GA group reached 100% (Fig. 6). We also observed reduced leukocyte influxes (Fig. 7a) and HMGB1 (Fig. 7b) levels in the BAL from LPS + GA mice compared with the LPS group ($p < 0.001$). ROS (Fig. 7c) and MCP-1 (Fig. 7d) were increased in the LPS group ($p < 0.01$ and $p < 0.05$) compared with the GA group. The ROS and MCP-1 of the LPS + GA group were not different from those of the GA group. CCR2 levels in the tissue from LPS mice were increased ($p < 0.05$) compared with control group (Fig. 7e). GA did not reduce CCR2 levels in LPS injected mice. Histological analyses of the lung, kidney and liver of LPS + GA mice (Fig. 8a–c) showed reduced leukocyte infiltration and tissue damage relative to the LPS mice (Fig. 3b, f and j). No differences were observed between the control group and the GA group for any of the analyses performed.

Discussion

In the present study, we demonstrated that the chemokine receptor CCR2 is important in the inflammatory events of experimental

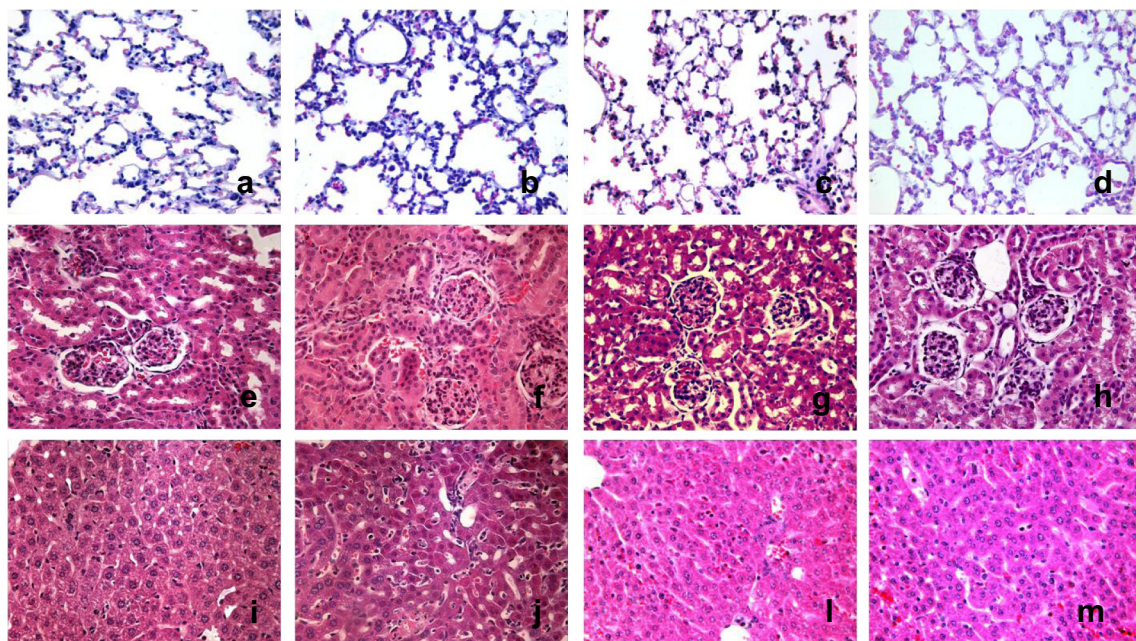


Fig. 3. Photomicrographs of lung (a–d), kidney (e–h) and liver (i–l). We observed congestion, haemorrhage and leukocytes on the lung parenchyma in WT mice (b) injected with LPS compared with the control group (a). The lung histology of CCR2 KO mice (d) injected with LPS was not different from that of the control group (c). The kidney tissue of WT mice (f) injected with LPS showed that renal tubular cells underwent significant vacuolar degenerative changes and leukocyte infiltrations in the glomeruli and interstitium compared with the control group (e). CCR2 mice injected with LPS (h) showed lesser kidney leukocyte infiltrations and no vacuolar degenerative changes compared with WT mice (g). The liver tissue of WT mice (j) injected with LPS showed wide-range laminated necrosis, acidophilia changes, and parenchyma leukocyte infiltrations compared with the control group (i). Liver tissue from CCR2 mice injected with LPS (l) showed only lesser parenchyma leukocyte infiltrations when compared with control group (k). 400 \times , H&E. ($n = 5$ per group).

sepsis via ERK 1/2 and HMGB1 expression, contributing significantly to the mortality observed during the first 24 h of endotoxic shock. At this point, CCR2 and HMGB1 could present important targets for the treatment of sepsis in its initial stages.

Sepsis is defined as a systemic inflammatory response to infection characterised by the deregulated production of proinflammatory cytokines [1]. Clinical trials have demonstrated that neutrophils in patients with sepsis express high levels of CCR2, and disease severity (SOFA scores and APACHE) correlated positively with the observed increase in neutrophil chemotaxis to MCP-1. These authors also conclude that inhibition of CCR2 signaling may be beneficial in patients with sepsis and multiple organ failure [28]. To test this hypothesis, we initially observed the survival dose–response curve in CCR2 knockout mice compared with wild type subjected to endotoxaemia, and we observed that there was greater mortality in the wild type mice. Maus and co-workers also demonstrated that the intratracheal administration of LPS

causes an inflammatory response of the amplifier CCR2 chemokine receptor after stimulation [29].

We used LPS as a promoter of endotoxaemia, which is responsible for the release of certain inflammatory cytokines, such as TNF- α , which is produced by monocytes/macrophages, T lymphocytes, natural killer cells and mast cells [3,8]. These cells induce increased expression of adhesion molecules in endothelial cells, expression and secretion of chemokines by macrophages, and expression of enzymes, such as cyclooxygenase-2 (COX-2) and NO-synthase (iNOS) [30–32]. TNF- α plays an important role in this complex pathophysiological response by stimulating leukocytes and endothelial cells to release other cytokines to express adhesion molecules on the cell surface and increase the turnover of arachidonic acid [33]. Therefore, we suggest that the increased expression of TNF- α may have been responsible for iNOS producing NO from L-arginine and for the metabolism of this NO to nitrite and nitrate. This response involving NO overproduction led to hypotension

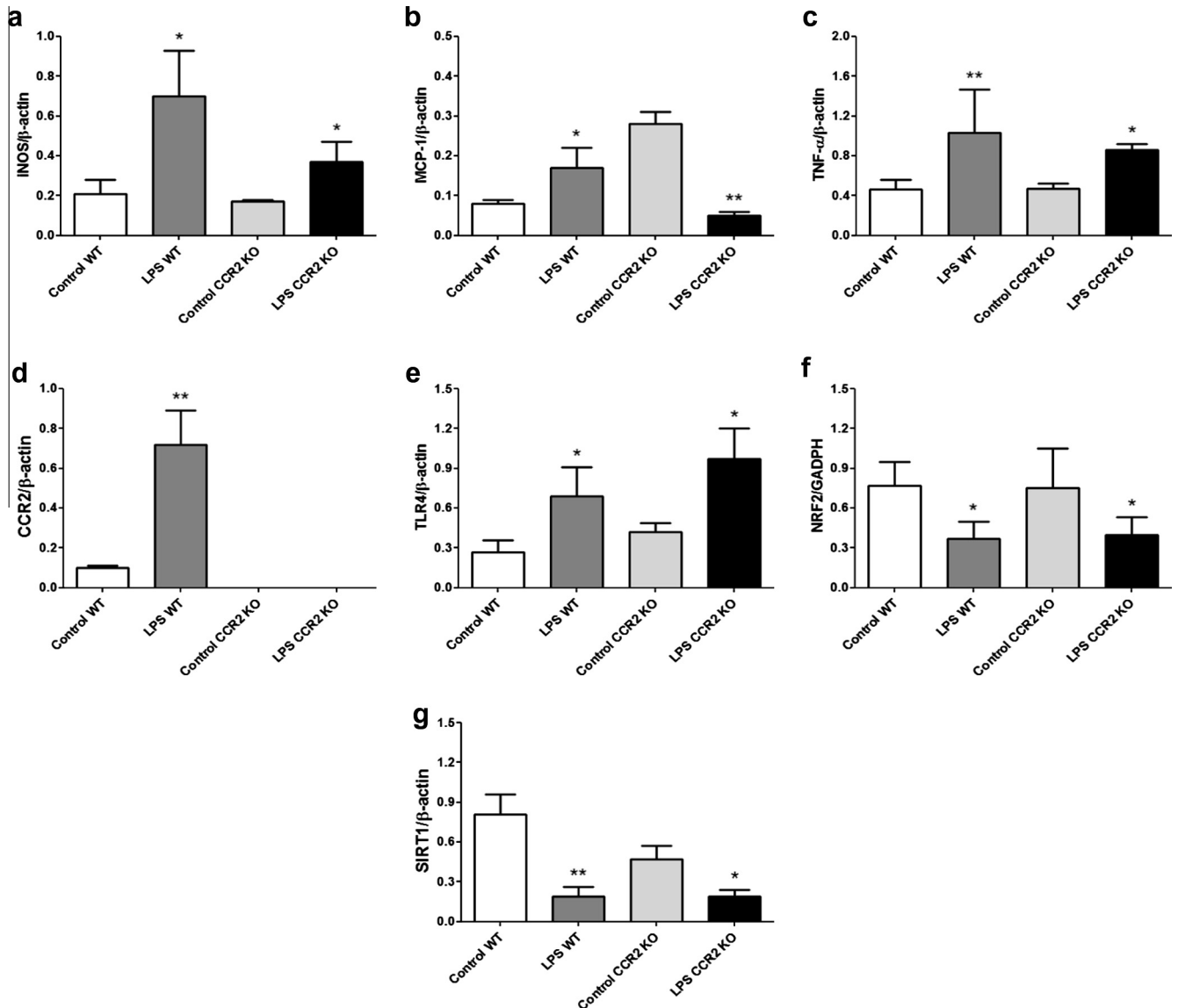


Fig. 4. The expression of inflammatory and redox markers in the lung homogenates of mice injected with LPS (20 mg/kg). (a) inducible isoform of nitric oxide synthase, (b) monocyte chemoattractant protein-1, (c) tumour necrosis factor alpha, (d) chemokine (C-C motif) receptor 2, (e) toll-like receptor 4, (f) nuclear factor (erythroid-derived 2)-like 2, and (g) sirtuin (silent mating type information regulation 2 homolog) 1. All of the analyses were normalised to a constitutively expressed gene (β -actin or hypoxanthine phosphoribosyl-transferase 1). The data were expressed as the means \pm SEM. The statistical analyses were performed by unpaired Student's *T* tests with Welch's correction, considering the significance level to be 5%. **p* < 0.05, ***p* < 0.01 and ****p* < 0.001 compared with the respective control group. *n* = 5 per group.

and refractory vasodilation in the mice, culminating in the mortality observed in the WT animals. The finding that the CCR2 knock-out mice showed lower levels of nitrite suggests a logical hypothesis regarding the role of NO metabolism in endotoxin shock-induced lethality. Interestingly, studies on septic patients and in septic mice have also demonstrated increased levels of nitrite and nitrate [34,35]. Moreover, Mitaka and co-workers showed that the levels of nitrite/nitrate in the plasma of septic patients are correlated with the severity of the syndrome and multiple organ dysfunctions, measured by APACHE II and SOFA scores, respectively [36].

The accumulation of neutrophils has been reported in the development of pulmonary sepsis, not only favouring bacterial translocation but also promoting the production of ROS [37]. Our study revealed elevated ROS and MPO in both WT mice and CCR2 KO mice. However, the CCR2 KO mice exhibited a less pronounced elevation of ROS and MPO than the WT mice, thus suggesting a degree of regulation of the oxidants produced by neutrophils through CCR2. In this context, the receptors involved in the mechanism of sepsis induced by LPS are the Toll-like receptors (TLRs) which mediate “scavenger” responses. Toll-like receptor 4 (TLR4), the receptor with the greatest importance in the

induction of sepsis by LPS, acts as a signalling centre for transcription factors for inflammation and redox responses [38].

In our study, increased expression of TLR4 detected in the two groups and thus can confirm the host response to the LPS stimulus. In sepsis, there are a variety of secreted chemokines, such as MCP-1, a protein that exerts an attraction for monocytes and macrophages by interacting with its surface receptor, CCR2 [22,28,29]. Several studies have shown that the levels of MCP-1 are increased in animal models of sepsis [10,39]. In our study, we have found a decrease in the expression of this chemokine in CCR2 KO mice, and we suggest that this decrease is due to a negative feedback mechanism in which the absence of CCR2 reduces MCP-1 and, consequently, mortality.

NRF2 is a transcription factor that is essential for the regulation of antioxidant enzymes. Mice deficient in NRF2 are sensitive to oxidative stress and inflammatory insults [40–44]. In our study, the expression of NRF2 was decreased in both groups exposed to endotoxaemia, and thus, we assume that the period of 24 h used for the endotoxaemia was insufficient to analyse the expression of NRF2.

Previous studies have reported that decreased activity of SIRT1 enhances the NF κ B signaling and enhances inflammatory responses [45,46]. Also, the overexpression of SIRT1 have been shown to disturb cellular redox balance by repressing the NRF2-induced antioxidant defense [47]. These data indicate a crosstalk with NF κ B system, suggesting that SIRT1 can not only repress the ROS production but also reduce the antioxidant defense. Interestingly, although both SIRT-1 and NRF2 expressions were decreased in mouse groups exposed to LPS, CCR2 KO mice showed lower inflammatory responses and lower ROS production when compared to WT mice.

We evaluated the role of CCR2 in the expression of HMGB1 as a major target in experimental sepsis. This DNA linker nuclear protein, present in both the nucleus and the cytoplasm or in the cytoplasmic membrane, is secreted by monocytes/macrophages and neutrophils after stimulation with LPS, IL-1 and TNF- α [18,20,48]. Several studies have demonstrated a central role of HMGB1 in organ dysfunction associated with severe sepsis. In patients with severe sepsis, as well as animals subjected to experimental models of sepsis, systemic levels of HMGB1 were elevated [49–54]. Nevertheless, neutralisation of this cytokine with antibodies protected the animals from lethal endotoxaemia and sepsis induced by the CLP model [55,56].

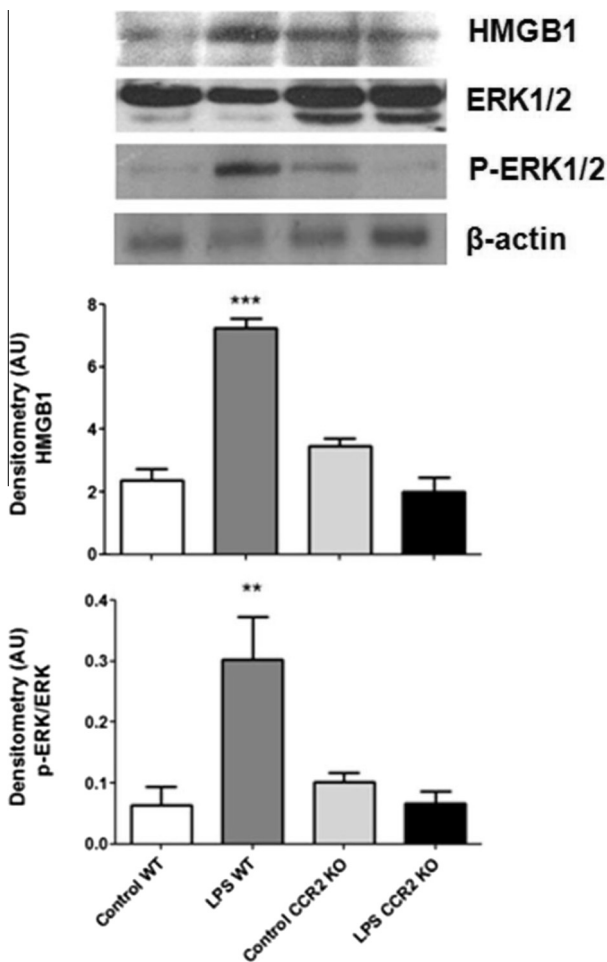


Fig. 5. Western blotting of HMGB1, ERK 1/2 and p-ERK 1/2. There is an increase in HMGB1 expression in the BAL of WT mice injected with LPS in comparison with the control group, whereas CCR2 KO mice injected with LPS were similar to the respective control group. At the same time point, we observed an increase in pERK 1/2 that paralleled a reduction in ERK 1/2 in WT mice injected with LPS. The pERK 1/2: ERK 1/2 ratio in CCR2 KO mice injected with LPS was similar to that of the respective control group. WB was repeated three times.

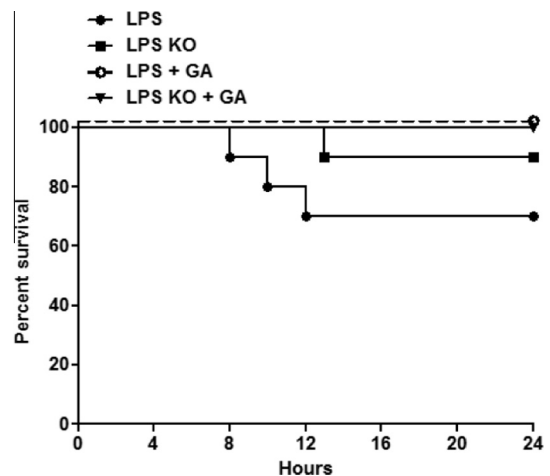


Fig. 6. Mouse survival after LPS-induced endotoxic shock. We observed that 100% of the LPS + GA and LPS KO + GA mice were alive 24 h into the experiment, whereas 10% of the mice in the LPS KO group and 30% of the mice in the LPS group were dead. GA-glycyrrhizic acid (50 mg/kg). These experimental designs were repeated two times. (n = 5 per group/time point).

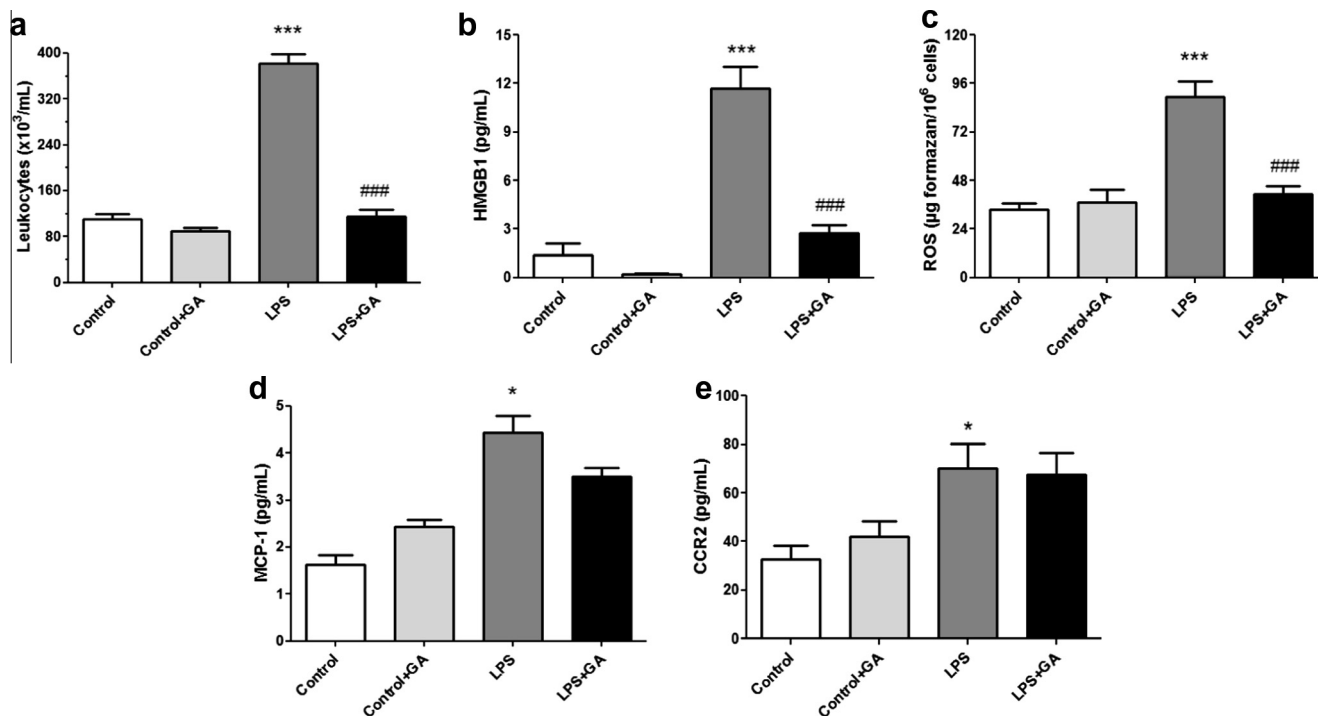


Fig. 7. Leukocytes, redox and proinflammatory markers from bronchoalveolar lavage of mice injected with LPS and treated with glycyrrhizic acid. (a) Total cells, (b) high mobility group box 1 protein, (c) reactive oxygen species, (d) monocyte chemoattractant protein 1, and (e) chemokine (C-C motif) receptor 2. GA-glycyrrhizic acid (50 mg/kg). The data were expressed as the means \pm SEM. The statistical analyses were performed by unpaired Student's *T* tests with Welch's correction, considering the significance level to be 5%. * $p < 0.05$ and *** $p < 0.001$ compared with the control group. ### $p < 0.001$ when compared with the LPS group. $n = 6$ per group.

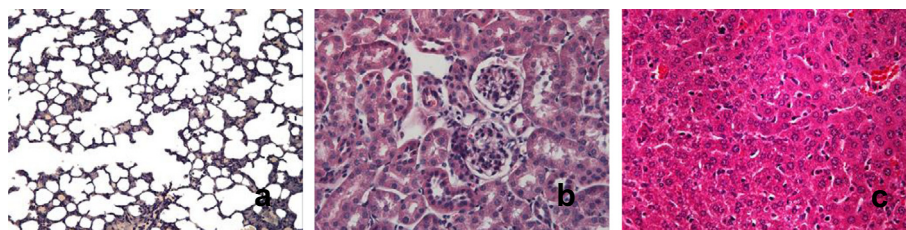


Fig. 8. Histological analyses of the lung, kidney and liver of LPS + GA mice (a, b and c) showed less leukocyte infiltration and tissue damage than was observed in LPS mice (Fig. 2b, f and j). GA-glycyrrhizic acid (50 mg/kg). 400 \times , H&E.

Another protein activated by LPS is phosphorylated ERK. This protein has two isoforms (ERK 1 and ERK 2), which are activated in the cascade of mitogen-activated protein kinase in response to endotoxin and oxidative stress, among other stimuli, and may be involved primarily in cell differentiation and proliferation [57]. The stimulation of macrophages in culture with MCP-1 rapidly induces the activation of ERK signalling as a promoter of the inflammatory response [58]. In addition, Lee and co-workers found that the activation of ERK has an important role in lung injury induced by LPS; therefore, their inhibition was significantly effective in reducing the cascade catalyst by reducing the leakage of protein and neutrophil influxes [6]. Thus, we suggest that, in our study, WT mice injected with LPS were more susceptible to the systemic effects of endotoxic shock and this effect was synergistic with the secretion of HMGB1.

We are the first group to demonstrate the importance of MCP-1/CCR2 in HMGB1 expression. Additionally, we confirmed the inhibition of HMGB1 expression by glycyrrhizic acid (GA), offering 100% protection against LPS-induced lethality in mice, and this final point suggests a critical role for HMGB1 in this model of endotoxic shock that mimics sepsis in humans. GA was the subject of several studies regarding its inflammatory context [59–61]. GA inhibits the

manifestation of anti-inflammatory responses that appear in association with systemic inflammatory response syndrome (SIRS)-like reactions [62]. We observed a reduction in the number of leukocytes in the mice injected with LPS and treated with GA, as well as reductions in HMGB1, ROS and MCP-1. Moreover, the histology of the lung, kidney and liver from these mice were similar to that of the control group. These facts help us to suggest a critical role for HMGB1 as a systemic marker of endotoxic shock induced by LPS in mice.

Glycyrrhizic acid is a known functional inhibitor of extracellular HMGB1 which has been reported to show anti-inflammatory properties [63]. Glycyrrhizic acid treatment has been shown to decrease both inflammation and infection in CLP-induced liver damage by regulating polymorphonuclear (PMN) chemoattraction, suggesting that it is likely that HMGB1 exerts its chemotactic function toward PMNs extracellularly [64]. The present study may shed some light in this matter as we are the first group to identify the association between CCR2 and HMGB1, as key LPS-induced pulmonary sepsis parameters were significantly reduced in mice treated with glycyrrhizic acid. Recently, the association between HMGB1 inhibition in macrophages has been shown to reduce the release of important inflammatory markers, such as prostaglandin E2 and TNF- α [65],

two key cytokines that are involved in LPS susceptibility and further increase of mouse in life [66]. In addition, HMGB1 inhibition has been shown to block cytokine expression via JNK/NF κ B pathway which led the authors to suggest HMGB-1 could act as a therapeutic target for inflammation, which is in accordance with the present study [67].

The lack of information regarding to the levels of ERK signals in treatment of glycyrrhizic acid represents a limitation of the present study. However, it is most likely that ERK signaling may also be reduced, as mouse life-span improvement shown in the present study, has been repeatedly shown to depend on ERK1/2 cascade inhibition and mice lacking the MKP-2 gene had a survival advantage over wild-type mice when challenged with LPS [68–70].

These facts help us to suggest a critical role for HMGB1 as a systemic marker of endotoxic shock induced by LPS in mice

Conclusions

In conclusion, we demonstrated that, after stimulation with LPS, CCR2 KO mice survive more frequently and exhibit altered inflammatory and redox profiles. These parameters were accompanied by the ERK 1/2 pathway and offered us the opportunity to investigate HMGB1 involvement in WT mice using an inhibitor. Three lessons can be highlighted from our study: (1) CCR2 and HMGB1 play critical roles in our endotoxic shock model, (2) the participation of chemokines related to monocytes/macrophages are as important as neutrophil responses for sepsis in mice, and (3) redox participation in CCR2 KO mice is quite limited, considering the inflammatory events. Thus, drugs that target CCR2 and HMGB1 could represent future resources for sepsis treatment in humans, particularly in the early stages of this condition.

Acknowledgments

The authors are grateful to the Brazilian research agencies FAPERJ, FAPESP, CAPES and CNPq for grants (to professors) and scholarships (to undergraduate and graduate students). We are grateful also to all undergraduate students from LABCOM for technical advices with biochemical analyses.

References

- [1] D.G. Remick, P.A. Ward, *Shock* 24 (Suppl. 1) (2005) 7–11.
- [2] M. Moss, *Clin. Infect. Dis.* 41 (Suppl. 7) (2005) S490–S497.
- [3] H.M. Razavi, L. Wang, S. Weicker, G.J. Quinlan, S. Mumby, D.G. McCormack, S. Mehta, *Crit. Care Med.* 33 (2005) 1333–1339.
- [4] L.F. Poli-de-Figueiredo, A.G. Garrido, N. Nakagawa, P. Sannomiya, *Shock* 30 (Suppl. 1) (2008) 53–59.
- [5] S. Leekha, H.C. Standiford, *Crit. Care Med.* 39 (2011) 1995–1996.
- [6] C. Lee, H.J. An, J.L. Kim, H. Lee, S.G. Paik, *Mol. Cells* 27 (2009) 251–255.
- [7] K. Tsoyi, T.Y. Lee, Y.S. Lee, H.J. Kim, H.G. Seo, J.H. Lee, K.C. Chang, *Mol. Pharmacol.* 76 (2009) 173–182.
- [8] V.M. Victor, M. Rocha, M. De la Fuente, *Int. Immunopharmacol.* 4 (2004) 327–347.
- [9] V.M. Victor, M. Rocha, J.V. Esplugues, M. De la Fuente, *Curr. Pharm. Des.* 11 (2005) 3141–3158.
- [10] R.D. Ramnath, S.W. Ng, A. Guglielmotti, M. Bhatia, *Int. Immunopharmacol.* 8 (2008) 810–818.
- [11] A.B. Reddy, S.K. Srivastava, K.V. Ramana, *Cytokine* 48 (2009) 170–176.
- [12] D. Tang, R. Kang, W. Xiao, H. Zhang, M.T. Lotze, H. Wang, X. Xiao, *Am. J. Respir. Cell Mol. Biol.* 41 (2009) 651–660.
- [13] M.A. van Zoelen, H. Yang, S. Florquin, J.C. Meijers, S. Akira, B. Arnold, P.P. Nawroth, A. Bierhaus, K.J. Tracey, T. van der Poll, *Shock* 31 (2009) 280–284.
- [14] L.Y. Gamez-Diaz, L.E. Enriquez, J.D. Matute, S. Velasquez, I.D. Gomez, F. Toro, S. Ospina, V. Bedoya, C.M. Arango, M.L. Valencia, G. De La Rosa, C.I. Gomez, A. Garcia, P.J. Patino, F.A. Jaimes, *Acad. Emerg. Med.* 18 (2011) 807–815.
- [15] A. Bitto, M. Barone, A. David, F. Polito, D. Familiari, F. Monaco, M. Giardina, T. David, R. Messina, A. Noto, V. Di Stefano, D. Altavilla, A. Bonaiuto, L. Minutoli, S. Guarini, A. Ottani, F. Squadrito, F.S. Venuti, *Pharmacol. Res.* 61 (2010) 116–120.
- [16] T. Hatada, H. Wada, T. Nobori, K. Okabayashi, K. Maruyama, Y. Abe, S. Uemoto, S. Yamada, I. Maruyama, *Thromb. Haemost.* 94 (2005) 975–979.
- [17] C. Bopp, A. Bierhaus, S. Hofer, A. Bouchon, P.P. Nawroth, E. Martin, M.A. Weigand, *Crit. Care* 12 (2008) 201.
- [18] G. Chen, M.F. Ward, A.E. Sama, H. Wang, J. Interferon Cytokine Res. 24 (2004) 329–333.
- [19] S. Dai, C. Sodhi, S. Cetin, W. Richardson, M. Branca, M.D. Neal, T. Prindle, C. Ma, R.A. Shapiro, B. Li, J.H. Wang, D.J. Hackam, *J. Biol. Chem.* 285 (2010) 4995–5002.
- [20] N.K. Sun, C.C. Chao, *Chang Gung Med. J.* 28 (2005) 673–682.
- [21] H. Wang, H. Yang, K.J. Tracey, *J. Intern. Med.* 255 (2004) 320–331.
- [22] W.A. Kuziel, S.J. Morgan, T.C. Dawson, S. Griffin, O. Smithies, K. Ley, N. Maeda, *Proc. Natl. Acad. Sci. USA* 94 (1997) 12053–12058.
- [23] M.M. Bradford, *Anal. Biochem.* 72 (1976) 248–254.
- [24] H.S. Choi, J.W. Kim, Y.N. Cha, C. Kim, *J. Immunoassay Immunochem.* 27 (2006) 31–44.
- [25] K. Suzuki, H. Ota, S. Sasagawa, T. Sakatani, T. Fujikura, *Anal. Biochem.* 132 (1983) 345–352.
- [26] L.C. Green, D.A. Wagner, J. Glogowski, P.L. Skipper, J.S. Wishnok, S.R. Tannenbaum, *Anal. Biochem.* 126 (1982) 131–138.
- [27] K.J. Livak, T.D. Schmittgen, *Methods (San Diego Calif)* 25 (2001) 402–408.
- [28] A. Kapoor, C. Thiemeermann, *Am. J. Respir. Crit. Care Med.* 183 (2011) 150–151.
- [29] U.A. Maus, S. Wellmann, C. Hampf, W.A. Kuziel, M. Srivastava, M. Mack, M.B. Everhart, T.S. Blackwell, J.W. Christman, D. Schlondorff, R.M. Bohle, W. Seeger, J. Lohmeyer, *Am. J. Physiol. Lung Cell. Mol. Physiol.* 288 (2005) L350–L358.
- [30] T. Uto, N. Suangkaew, O. Morinaga, H. Kariyazono, S. Oiso, Y. Shoyama, *Am. J. Chin. Med.* 38 (2010) 985–994.
- [31] P. Pratheeshkumar, G. Kuttan, *Immunopharmacol. Immunotoxicol.* 33 (2011) 73–83.
- [32] H.S. Chae, O.H. Kang, Y.S. Lee, J.G. Choi, Y.C. Oh, H.J. Jang, M.S. Kim, J.H. Kim, S.I. Jeong, D.Y. Kwon, *Am. J. Chin. Med.* 37 (2009) 181–194.
- [33] Y. Tanaka, A. Otsuji, F. Amano, *Biol. Pharm. Bull.* 22 (1999) 1052–1057.
- [34] J.P. Cobb, R.L. Danner, *JAMA* 275 (1996) 1192–1196.
- [35] D. Le Roy, D. Heumann, M.P. Glauser, J. Mauel, J. Smith, S. Betz Corradin, *Shock* 10 (1998) 37–42.
- [36] C. Mitaka, Y. Hirata, K. Yokoyama, H. Wakimoto, M. Hirokawa, T. Nosaka, T. Imai, *Shock* 19 (2003) 305–309.
- [37] Y. Wang, C. Bai, X. Wang, *Expert Rev. Respir. Med.* 2 (2008) 297–299.
- [38] E.F. Kenny, L.A. O'Neill, *Cytokine* 43 (2008) 342–349.
- [39] R.N. Gomes, R.T. Figueiredo, F.A. Bozza, P. Pacheco, R.T. Amancio, A.P. Laranjeira, H.C. Castro-Faria-Neto, P.T. Bozza, M.T. Bozza, *Shock* 26 (2006) 457–463.
- [40] J.Y. Choi, M.J. Kwun, K.H. Kim, J.H. Lyu, C.W. Han, H.S. Jeong, K.T. Ha, H.J. Jung, B.J. Lee, R.T. Sadikot, J.W. Christman, S.K. Jung, M. Joo, *Evid Based Complement Alternat. Med.* 2012 (2012) 974713.
- [41] F. Khodagholi, S.K. Tusi, *Mol. Cell. Biochem.* 354 (2011) 97–112.
- [42] K. Koh, J. Kim, Y.J. Jang, K. Yoon, Y. Cha, H.J. Lee, *J. Neuroimmunol.* 233 (2011) 160–167.
- [43] H. Wang, T.O. Khor, C.L. Saw, W. Lin, T. Wu, Y. Huang, A.N. Kong, *Mol. Pharm.* 7 (2010) 2185–2193.
- [44] R.K. Thimmulappa, C. Scollick, K. Traore, M. Yates, M.A. Trush, K.T. Liby, M.B. Sporn, M. Yamamoto, T.W. Kensler, S. Biswal, *Biochem. Biophys. Res. Commun.* 351 (2006) 883–889.
- [45] F. Yeung, J.E. Hoberg, C.S. Ramsey, M.D. Keller, D.R. Jones, R.A. Frye, M.W. Mayo, *EMBO J.* 23 (2004) 2369–2380.
- [46] A. Salminen, J.M. Hyttinen, K. Kaarniranta, *J. Mol. Med. (Berl)* 89 (2011) 667–676.
- [47] Y. Kawai, L. Garduno, M. Theodore, J. Yang, I.J. Arinze, *J. Biol. Chem.* 286 (2010) 7629–7640.
- [48] H. Wang, O. Bloom, M. Zhang, J.M. Vishnubhakat, M. Ombrellino, J. Che, A. Frazier, H. Yang, S. Ivanova, L. Borovikova, K.R. Manogue, E. Faist, E. Abraham, J. Andersson, U. Andersson, P.E. Molina, N.N. Abumrad, A. Sama, K.J. Tracey, *Science* 285 (1999) 248–251.
- [49] W. Huang, Y. Tang, L. Li, *Cytokine* 51 (2010) 119–126.
- [50] H. Wang, M.F. Ward, A.E. Sama, *Shock* 32 (2009) 348–357.
- [51] H. Wang, S. Zhu, R. Zhou, W. Li, A.E. Sama, *Expert Rev. Mol. Med.* 10 (2008) e32.
- [52] S. Karlsson, V. Pettila, J. Tenhunen, R. Laru-Sompa, M. Hynninen, E. Ruokonen, *Intensive Care Med.* 34 (2008) 1046–1053.
- [53] G.W. Waterer, *Crit Care Med* 35 (2007) 1205–1206.
- [54] S. Qin, H. Wang, R. Yuan, H. Li, M. Ochani, K. Ochani, M. Rosas-Ballina, C.J. Czura, J.M. Huston, E. Miller, X. Lin, B. Sherry, A. Kumar, G. Larosa, W. Newman, K.J. Tracey, H. Yang, *J. Exp. Med.* 203 (2006) 1637–1642.
- [55] J. Li, H. Wang, J.M. Mason, J. Levine, M. Yu, L. Ulloa, C.J. Czura, K.J. Tracey, H. Yang, *J. Immunol. Methods* 289 (2004) 211–223.
- [56] G. Chen, J. Li, X. Qiang, C.J. Czura, M. Ochani, K. Ochani, L. Ulloa, H. Yang, K.J. Tracey, P. Wang, A.E. Sama, H. Wang, *J. Lipid Res.* 46 (2005) 623–627.
- [57] D. Strassheim, J.S. Park, E. Abraham, *Int. J. Biochem. Cell Biol.* 34 (2002) 1527–1533.
- [58] A. Sodhi, S.K. Biswas, *J. Interferon Cytokine Res.* 22 (2002) 517–526.
- [59] W. Arjumand, S. Sultana, *Life Sci.* 89 (2011) 422–429.
- [60] J.M. Cherng, K.D. Tsai, Y.W. Yu, J.C. Lin, *Radiat. Res.* 176 (2011) 177–186.
- [61] Y. Liu, J. Xiang, M. Liu, S. Wang, R.J. Lee, H. Ding, *J. Pharm. Pharmacol.* 63 (2011) 439–446.
- [62] M. Takei, M. Kobayashi, D.N. Herndon, R.B. Pollard, F. Suzuki, *Cytokine* 35 (2006) 295–301.
- [63] L. Mollica, F. De Marchis, A. Spitaleri, C. Dallacosta, D. Pennacchini, M. Zamai, A. Agresti, L. Trisciuglio, G. Musco, M.E. Bianchi, *Chem. Biol.* 14 (2007) 431–441.

- [64] G. Sitia, M. Iannacone, S. Muller, M.E. Bianchi, L.G. Guidotti, *J Leukoc Biol* 81 (2007) 100–107.
- [65] W. Wang, M. Luo, Y. Fu, S. Wang, T. Efferth, Y. Zu, *Int. J. Nanomedicine* 8 (2013) 1377–1383.
- [66] S.N. Vogel, C.T. Hansen, D.L. Rosenstreich, *J. Immunol.* 122 (1979) 619–622.
- [67] X. Wu, Y. Mi, H. Yang, A. Hu, Q. Zhang, C. Shang, *Mol. Cell. Biochem.* (2013) 12–15.
- [68] T.T. Cornell, P. Rodenhouse, Q. Cai, L. Sun, T.P. Shanley, *Infect Immun* 78 (2010) 2868–2876.
- [69] H. Fan, B. Zingarelli, V. Harris, G.E. Tempel, P.V. Halushka, J.A. Cook, *Mol. Med.* 14 (2008) 422–428.
- [70] H. Li, Y. Wang, H. Zhang, B. Jia, D. Wang, D. Lu, R. Qi, Y. Yan, H. Wang, *PLoS One* 7 (2012) e52863.